Journal of Structural Biology 213 (2021) 107705

Contents lists available at ScienceDirect

Journal of Structural Biology

journal homepage: www.elsevier.com/locate/yjsbi

The ultrastructure of resurrection: Post-diapause development in an Antarctic freshwater copepod

Katherine A. Reed [a], Sung Gu Lee [b,c], Jun Hyuck Lee [b,c], Hyun Park [d], Joseph A. Covi [a,*]

[a] The University of North Carolina at Wilmington, Department of Biology and Marine Biology, 601 S. College Rd., Wilmington, NC 28403, USA
[b] Unit of Research for Practical Application, Korea Polar Research Institute (KOPRI), Yeonsu-gu, Incheon 21990, South Korea
[c] Department of Polar Sciences, University of Science and Technology, Incheon 21990, South Korea
[d] Division of Biotechnology, Korea University, 145 Anam-ro, Seungbuk-gu, Seoul, South Korea

ARTICLE INFO

Keywords:
Crustacean
Zooplankton
Diapause
Developmental biology
Partial syncytium
Electron microscopy

ABSTRACT

The copepod, *Boeckella poppei,* is broadly distributed in Antarctic and subantarctic maritime lakes threatened by climate change and anthropogenic chemicals. Unfortunately, comparatively little is known about freshwater zooplankton in lakes influenced by the Southern Ocean. In order to predict the impact of climate change and chemicals on freshwater species like *B. poppei*, it is necessary to understand the nature of their most resilient life stages. Embryos of *B. poppei* survive up to two centuries in a resilient dormant state, but no published studies evaluate the encapsulating wall that protects theses embryos or their development after dormancy. This study fills that knowledge gap by using microscopy to examine development and the encapsulating wall in *B. poppei* embryos from Antarctica. The encapsulating wall of *B. poppei* is comprised of three layers that appear to be conserved among crustacean zooplankton, but emergence and hatching are uniquely delayed until the nauplius is fully formed in this species. Diapause embryos in Antarctic sediments appear to be in a partially syncytial mid-gastrula stage. The number of nuclei quadruples between the end of diapause and hatching. Approximately 75% of yolk platelets are completely consumed during the same time period. However, some yolk platelets are left completely intact at the time of hatching. Preservation of complete yolk platelets suggests an all-or-none biochemical process for activating yolk consumption that is inactivated during dormancy to preserve yolk for post-dormancy development. The implications of these and additional ultrastructural features are discussed in the context of anthropogenic influence and the natural environment.

1. Introduction

In order to predict how lake ecosystems in the Antarctic and subantarctic will change over time, we must first understand the most resilient life-stages of critically important species in these lakes. A small number of endemic crustacean zooplankton and rotifers occupy the apex of simple food webs in Antarctic lakes (Laybourn-Parry and Pearce, 2007). While some Antarctic lakes may have active zooplankton populations year-round (Laybourn-Parry et al., 2003), dormant life-stages are likely required for overwintering in shallow lakes that freeze completely during the austral winter. Crustacean zooplankton in inland lake and estuarine environments produce diapause eggs that resurrect after months to centuries of dormancy (Hairston and Cáceres, 1996; Jiang et al., 2012; Marcus et al., 1994). The importance of these dormant "egg banks" in maintaining zooplankton populations is well documented (Brendonck and De Meester, 2003; Hairston and Kearns, 2002; Marcus and Boero, 1998; Cáceres and Hairston, 1998). However, despite the critical role dormant embryos play in maintaining zooplankton populations, relatively little is known about the ultrastructure of dormant embryos and post-dormancy development in freshwater calanoid copepods from any environment. Embryos of the calanoid copepod, *Boeckella poppei*, survive for nearly 200 years in the sediments of freshwater lakes on King George Island, South Shetland Islands, Antarctica (Jiang et al., 2012). The extreme longevity of their dormant embryos, and requirement for an overwintering life-stage, suggests that dormancy is a crucial life history strategy for *B. poppei* found in shallow Antarctic lakes. The present study fills a large knowledge gap by providing the first ultrastructural evaluation of dormant embryos and post-dormancy development in a calanoid copepod. It is also the first study of post-diapause development in a crustacean zooplankton from freshwater lakes influenced by the

* Corresponding author.
E-mail address: covij@uncw.edu (J.A. Covi).

https://doi.org/10.1016/j.jsb.2021.107705
Received 11 September 2020; Received in revised form 27 January 2021; Accepted 29 January 2021
Available online 9 February 2021

Southern Ocean. As such, the data presented here provides a developmental foundation for future research on freshwater copepods.

Encysted embryos of diverse zooplankton from inland waters, including *B. poppei*, experience multiple forms of cryptobiotic dormancy before hatching. Diapause is a dormant state that is developmentally programmed, and must be broken (terminated) by an environmental cue for development to continue (Alekseev et al., 2007; Clegg et al., 1996; Hand and Podrabsky, 2000). *Boeckella triarticulata* produces verified diapause embryos that are distinguishable from non-diapause embryos with transmission electron microscopy (Couch et al., 2001). Antarctic *B. poppei* also appear to produce true diapause embryos. As evidence of this, few *B. poppei* embryos hatch within the first two weeks after isolation from lake sediment, and exposure to light under aerobic conditions increases hatching (Reed et al., 2018). After breakage of the diapause state, development in *B. poppei* is suspended again by exposure to anoxia (Reed et al., 2018). This form of anoxia-induced dormancy is referred to as quiescence (Hand and Podrabsky, 2000). Because *B. poppei* is capable of both diapause and quiescence, it is possible that embryos may be in either form of dormancy when isolated from Antarctic lake sediments. However, few embryos hatch within the first two weeks after isolation from sediment that was stored in the dark at 4 °C, and <50% of embryos hatch within one month of isolation (Reed et al., 2018). This delayed hatching profile is consistent with diapause, and suggests that the *B. poppei* embryos used by Reed et al. (2018) were almost exclusively in a state of diapause upon isolation from the sediment.

Research on the development of crustacean zooplankton was popular in the late 1880s to the early 1960s. Now, more than a century since this field started, we still lack a clear comparative understanding of embryonic structure during dormancy and the changes that occur after resurrection from the dormant state. Most morphological studies on diapause embryos use anostracan models (Morris and Afzelius, 1967; Rosowski et al., 1997; Sugumar and Munuswamy, 2006), with some additional work in cladoceran species (Seidman and Larsen, 1979; Stout, 1956) and marine copepods (Chen and Marcus, 1997; Ianora and Santella, 1991; Santella and Ianora, 1990). Ultrastructural research on freshwater species focused primarily on either distinguishing immediately hatching embryos (subitaneous) from diapause embryos of the same species (Couch et al., 2001; Hairston and Olds, 1984) or on the formation of the egg envelope during oogenesis (Cuoc et al., 1994). Few published studies include observations during diapause or post-diapause development in freshwater copepods, and there are no published data on ultrastructural changes during post-diapause development in any Antarctic species.

In all species for which morphological data exist, diapause embryos of zooplankton are surrounded by an encapsulating cyst wall that includes three to four distinct layers (Couch et al., 2001; Cuoc et al., 1994; Dharani and Altaff, 2004; Hairston and Olds, 1984; Hirose et al., 1992; Hubble and Kirby, 2007; Ianora and Santella, 1991; Rosowski et al., 1997; Santella and Ianora, 1990; Seidman and Larsen, 1979). This complex barrier provides protection against mechanical and chemical insults until emergence, which is when exit from the cyst wall leaves the embryo surrounded only by a thin cuticle sometimes referred to as the hatching membrane (Morris and Afzelius, 1967; Rosowski et al., 1997; Reed et al., 2018). At hatching, a fully formed nauplius larva exits the hatching membrane (Morris and Afzelius, 1967; Rosowski et al., 1997; Reed et al., 2018).

Lakes influenced by the Southern Ocean provide the last relatively pristine environments in which to study freshwater zooplankton, but climate change and increased human activity in the Southern Ocean and Antarctica pose threats to the species found in these lakes. *Boeckella poppei* is an important model for research on freshwater zooplankton influenced by the Southern Ocean because it has a broad distribution that spans from the Antarctic continent to South America (Bayly, 1995; Bayly et al., 2003; Díaz et al., 2019; Maturana et al., 2019). It also occupies the highest trophic level of relatively simple food webs (Izaguirre et al., 2003; Pociecha and Dumont, 2008) and its dormant embryos are permeable to lipophilic chemicals (Reed et al., 2018). The primary objective of this study was to provide an ultrastructural foundation for future research on an important Antarctic species threatened by a rapidly changing climate and increasing human activity at higher latitudes of the southern hemisphere. A secondary objective was to fill a large gap in the understanding of diapause and post-diapause development in copepods.

2. Material & methods

2.1. Chemicals

All solutions were prepared using ultrapure deionized water (resistivity ≥ 18 MΩ cm at 25 °C). Food-grade sucrose was used to prepare solutions for density-dependent isolation of dormant zooplankton from sediments. Instant Ocean® artificial sea salts (Spectrum Brands, Blacksburg, VA, USA) were used to prepare artificial seawater (ASW) as a stock solution, which was later diluted to produce artificial freshwater (AFW). All other chemicals used in the isolation, preincubation and culturing of zooplankton were of ACS grade, EM grade, or higher.

2.2. Preparation of solutions for culturing of zooplankton

Stock solutions of 3.5‰ ASW were prepared, and salinity was determined with a refractometer (Vee Gee Scientific, Kirkland, WA, USA) at room temperature (approximately 22 °C) before dilution to 0.35‰ AFW as a working solution. All stock and working solutions were sterilized by vacuum filtration through a 0.2 μm polyethylsulfone (PES) filter and stored at 4 °C in sterile glass bottles until use.

2.3. Origin and preparation of zooplankton

A hand-operated stainless steel grab sampler (Wildco®, Yulee, FL, USA; product number 623-3110) was used to collect sediment samples containing dormant embryos of the Antarctic copepod, *B. poppei* without disturbing the surrounding sediments. Samples were collected from one maritime lake on Barton Peninsula, King George Island, Antarctica, (62.239869°S, 58.744733°W) in January 2016, February 2018 and February 2019 from a water depth of approximately 2 m in the limnetic zone of the lake. Sediment from a single grab was gently mixed to homogeneity and then divided into aliquots of approximately 30 mL. Aliquots were stored in Whirl-pak® bags (Nasco, Fort Atkinson, WI, USA). Therefore, each aliquot contains embryos from all depths captured in the sediment grab sample (approximately the top 5 cm of sediment). Aliquots from individual sediment grab samples were then placed in a 3.8 L Ziploc® bag to recreate bulk storage conditions that minimize surface area for gas exchange and light exposure. The maximum temperature recorded for all samples during shipment was 9 °C. Unless otherwise stated, sediment samples were stored at 4 °C and shielded from light until use. All procedures for processing of sediment samples were performed under dim red light provided by a 25 W 120 V incandescent bulb with opaque coating (Feit Electric Company, Pico Rivera, CA) in an environmental control room that maintained air temperature at 3.48 ± 0.01 °C, range 2.09 °C–5.24 °C.

Dormant embryos were separated from lake sediment using a modified version of the sugar floatation method described by Briski et al (2013). In brief, 5 mL of sediment was added to 45 mL of 80% sucrose, mixed by gentle inversion and centrifuged for 2 min at 1000 rcf with centrifuge chamber temperature maintained between 0 °C and 5 °C. The supernatant, which contained the zooplankton embryos, was then poured over a 63 μm stainless steel sieve. In order to remove residual sucrose, embryos were rinsed on the sieve with 500 mL of the 0.35‰ AFW solution used for culturing. Embryos were washed into a petri dish with 0.35‰ AFW solution for visual examination.

2.4. Characterization of developmental stage by light microscopy

Following isolation from the sediment, embryos were examined at 100X magnification under a Nikon SMZ745T dissecting microscope with G-AL 2X auxiliary lens (Nikon, Sterling Heights, MI, USA). *Boeckella poppei* were assigned to one of three developmental categories based on color and structural characteristics: Early Development (ED), Intermediate Development (ID), or Pre-Nauplius (PN) (Reed et al., 2018). Diapause occurs in the ED stage of development (Reed et al., 2018). Few embryos progressed beyond the ED stage before isolation from sediments. To obtain embryos at the ID and PN stages, 20–25 ED embryos were placed in each well of a sterile Cellstar® 12-well polystyrene culture plate (Greiner bio-one, Monroe, NC, USA) containing 1 mL of sterile 0.35‰ AFW. Development was monitored daily, and embryos of the ID and PN stages were collected approximately 7 d and 14 d respectively after isolation from native sediment. Representative images of embryos in each developmental category were captured at 100x magnification.

2.5. Evaluation of ultrastructural features using transmission electron microscopy

Ultrastructure was evaluated by transmission electron microscopy (TEM). Fixation of *B. poppei* for TEM was conducted according to the standard fixation method of Couch et al. (2001) with slight modification. In brief, approximately 10 individuals were fixed at one time in 1 mL of fixative consisting of 3% glutaraldehyde and 3% paraformaldehyde with 0.1 M phosphate buffer (pH = 7.4). Fixation was conducted at 4 °C for 24 h. To ensure penetration of fixative through the cyst wall, the samples were moved to room temperature for an additional 48 h. After fixation, *B. poppei* were rinsed three times with 0.1 M phosphate buffer (pH = 7.4), and left in the final phosphate buffer overnight. The *B. poppei* were post-fixed for 2 h in 1% osmium tetroxide with potassium ferrocyanide, rinsed three times in 0.1 M phosphate buffer (pH = 7.4), and remained in the final phosphate buffer rinse overnight. The following morning, *B. poppei* were placed in deionized water where they remained for 24 h. Next, *B. poppei* were block-stained with 2% uranyl acetate for 1 h, and then dehydrated by sequential incubation in 50%, 70%, and 95% EtOH; 45 min at each concentration. Complete dehydration was accomplished by incubation in 100% EtOH for 30 min, followed by two additional 100% EtOH washes of 60 min each. After dehydration, *B. poppei* were placed in propylene oxide for 30 min, then 60 min. Following propylene oxide treatment, *B. poppei* were placed into a 1:1 combination of propylene oxide:Spurr's resin (Spurr, 1969) overnight, then processed into a 1:3 combination for 2 h under vacuum to ensure penetration of the cyst wall. Samples were placed in fresh 100% Spurr's resin for 30 h under vacuum to ensure penetration. Resin was replaced six times during the 30 h treatment. Samples were then embedded and polymerized at 60 °C for 48 h.

All polymerized blocks were trimmed on a Reichert-Jung (Leica) Ultra-cut E Microtome (Labequip Ltd., Markham, Ontario, Canada). Thin sections (90 nm) of blocks were cut using a diamond knife (Micro Engineering Inc., Huntsville, TX, USA; serial #2044, 3.0 mm, 4°) and mounted on copper formvar support grids (Electron Microscopy Sciences, Hatfield, PA, USA). The thin sections were stained with 2% uranyl acetate and Reynolds lead citrate (Reynolds, 1963). High-resolution imaging was achieved using a Tecnai 12 Spirit (FEI Inc., Hillsboro, OR, USA) TEM with ion beam set to 80 KeV in brightfield mode. Images were cropped to areas of interest and labeled using Adobe Creative Cloud® 2020 software (Adobe Systems Incorporated, San Jose, CA, USA). Scale bars were included in all original micrographs, but occasionally cropped out or shifted in final figures.

Yolk platelets and nuclei were quantified using thick (1 μm) or semi-thick (0.5 μm) sections that were mounted on slides, stained with 0.1% toluidine blue following a modified protocol (Burns, 1978). Each section was stained with toluidine blue for 0.5 min–1.5 min on the medium setting of a hot plate (PC-220, Corning Incorporated, Corning, NY, USA) until the edges of the stain hardened. Slides were then rinsed with deionized water until water ran clear in order to remove excess stain. Stained sections were imaged using an Olympus BX60F-3 microscope (Olympus America Ltd., Center Valley, PA, USA) with a SPOT RT KE digital camera (SPOT Imaging, Diagnostic Instruments, Inc., Sterling Heights, MI, USA). Overview images for representative individuals of each developmental category were stitched together using Adobe Photoshop CC® 2015 software (Adobe Systems Incorporated, San Jose, CA, USA) to generate high-resolution images of whole transverse sections. Yolk platelets were identified by their spherical structure and uniquely homogenous dark appearance. Nuclei were identified by the distinct membrane and internal euchromatin and heterochromatin. Nuclei were counted using the TrakEM2 program of FIJI (Schindelin et al., 2012). Sequential thick sections (0.5 μm or 1 μm) were cut of the entire individual animal. Each nucleus was numbered and tracked by comparison of successive sections to prevent double-counting. It is important to note that the first and final 10 μm could not be sectioned without major artifacts or loss of entire section. Internal sections were also occasionally lost due to processing artifacts. Total nuclei (nuclei individual^{-1}) were determined from imaged sections and then scaled to the entire individual to account for the internal mass that could not be imaged. This scaling was accomplished by dividing the total number of nuclei in all imaged sections by the total volume of all imaged sections and then multiplying this quotient by the total volume of the sectioned embryo. Volume of a single section was calculated as a cylinder with section thickness as height. Total volume of the sectioned embryo was calculated using the equation for a sphere with a mean radius from the widest section.

The relative volume of all yolk platelets (yolk μm^{-3}) in an individual was also determined using the TrakEM2 program of FIJI. In brief, images of sections were imported to the program, and section thickness was entered. The cross-sectional area of yolk platelets was marked in each section using the Area List feature. Yolk platelets with a diameter equal to or greater than 0.5 μm were included in volume determination. Structures smaller than 0.5 μm were excluded from counts of yolk platelets because identity was difficult to confirm. The total cross-sectional area of yolk platelets was multiplied by the total thickness of all sections used to evaluate volume of yolk for each individual. The largest cross-sectional diameter was used to determine total volume of an individual, and the value for yolk volume was scaled to the entire individual. Nuclear count and yolk platelet volume were averaged for 5 individuals at the ED stage and 4 individuals each at the ID and PN stages.

2.6. Data analysis

A true replicate was considered to be a single *B. poppei*. Statistical analysis of the number of nuclei and yolk platelet volume was completed using JMP Pro 14.01.1 (SAS Institute, Cary, NC, USA). Homogeneity of variance was determined with a Levene's test. A Welch ANOVA ($\alpha = 0.05$) was employed on the $\log_{10}$ transformed datasets for mean nuclear count and yolk platelet volume, because the assumption of homogeneity of variance was not met for either dataset. A Games-Howell test was used for further post-hoc analysis.

3. Results

3.1. Characterization of post-diapause development of B. poppei

Early development in *B. poppei* was evaluated with light microscopy at 100X magnification in order to assign individuals to one of three pre-emergent categories (Fig. 1). A schematic diagram was then generated based on these images (Fig. 2a-c) and previously published micrographs (Reed et al., 2018). A summary of terms and major structural features was provided (Supplemental Table 1). Immediately following isolation from the sediment, the majority of embryos of *B. poppei* were in the Early

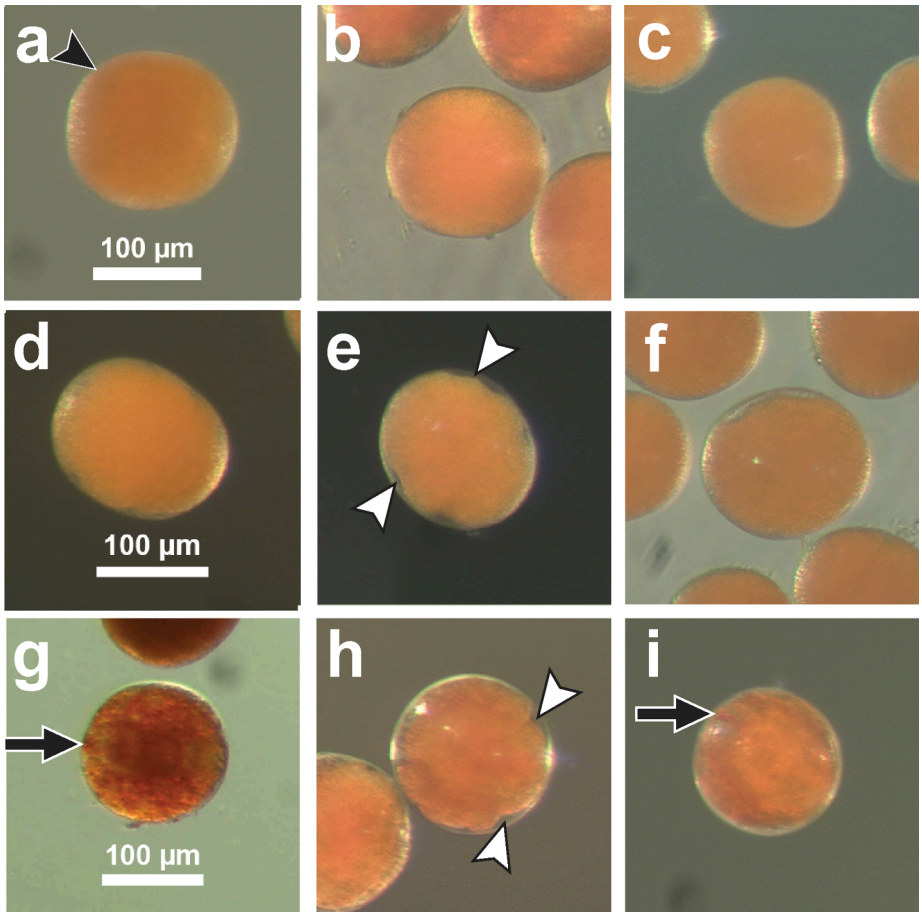

Fig. 1. Representative light-micrographs for the identification of Early Development (ED), Intermediate Development (ID) and Prenauplius (PN) stages of post-diapause development in *B. poppei* when viewed with a dissecting microscope at 100X magnification: (a-c) ED, (d-f) ID, and (g-i) PN. Internal mass appears homogenous with orange color in ED stage. No spaces are visible (a; black arrowhead) between the internal cell mass and the cyst wall in the ED stage. Segmentation furrows between the orange cell mass and cyst wall appear in the ID stage (e; white arrows). Variation in orange tone, a dark red ocellus (g,i; black arrow) and deep furrows with distinct borders on all sides (h; white arrow heads) are present in the early PN stage, but the furrows are difficult to distinguish late in the PN stage (g,i).

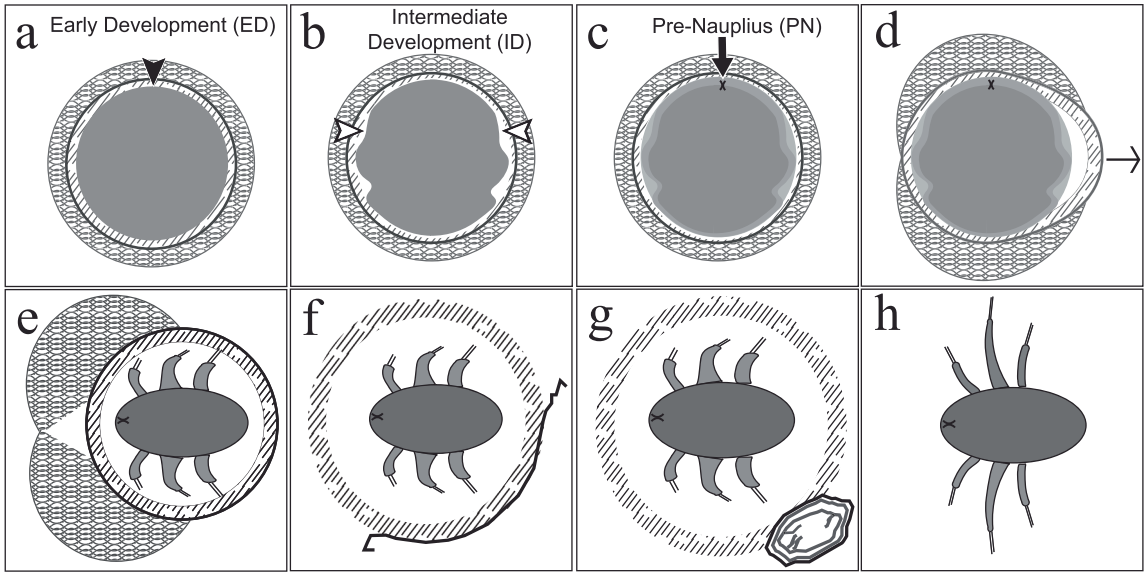

Fig. 2. Schematic diagrams emphasizing gross morphological characteristics needed for stage identification in post-diapause *B. poppei*. Normal progression includes three stages before hatching commences: (a) ED, where no space is visible between the cell mass and the cyst wall (black arrowhead), (b) ID where furrows appear typically in a bilaterally symmetrical fashion with space visible (white arrowheads) and (c) PN where an ocellus (black arrow) is typically visible. During emergence (d-g), the hatching membrane expands until (h) it ruptures at hatching and the nauplius swims free. Diagrams follow the morphology visible in the light images of Fig. 1 adapted from Reed et al. (2018) and Fig. 1 of this publication.

Development (ED) stage (Fig. 1a-c), with no differentiation of the embryonic mass visible by light microscopy. There were no spaces between the internal embryonic mass and the surrounding cyst wall at the ED stage. As embryos progressed to the Intermediate Development (ID) stage, furrows became apparent at the outer edge of the cell mass and this revealed a space between the cell mass and cyst wall (Fig. 1d-f). The

furrows were bilaterally symmetrical, but visibility of this symmetry depended on the viewing angle. The body wall is not well defined in the furrows observed in the ID stage. The embryonic mass retained its uniform red/orange color from the ED to the ID stage. Bilaterally symmetrical furrows deepened in the Pre-Nauplius (PN) stage (Fig. 1h), but prominence of the furrows varied with viewing angle (Fig. 1g-i). Variable shades of red and orange first appeared in the PN stage. At this point in development, a dark red ocellus was typically distinguishable.

The size of the embryo was constant prior to emergence. The mean diameter of ED, ID and PN stages was 143.65 μm ± 1.55 μm (n = 16), 144.97 ± 2.39 μm (n = 17), and 148.2 ± 2.01 μm (n = 18), respectively. The diameter did not change significantly between the ED stage and initiation of emergence at the end of the PN stage (one way ANOVA; $p = 0.123$).

3.2. Cyst wall ultrastructure during post-diapause development

A complex encapsulating cyst wall remained fully intact until the nauplius larva was fully developed (Fig. 3). The cyst wall of the post-diapause embryo was composed of three distinct layers distinguishable by TEM (Fig. 4). A thin outer layer (OL) with an average thickness of 0.04 ± 0.01 μm (n = 10) was present on the outermost edge of the cyst wall. A lamellar layer (LL) with an average thickness of 2.2 ± 0.01 μm (n = 10) was always present immediately under (proximal to) the OL. The third and innermost layer was designated as the inner membrane (IM), and had a thickness of 0.25 ± 0.01 μm (n = 10). The OL, LL, and IM layers maintain their structure throughout pre-emergent development (Fig. 4).

Two additional layers were identified under (proximal to) the IM in the PN stage that were not present in either the ED or ID stage. A second embryonic cuticle (EC2) appeared as a thin and highly folded membranous structure between a distal electron dense portion of the IM, and a proximal and less electron dense layer identified as the naupliar cuticle (Fig. 4c). The EC2 formed before the naupliar cuticle was complete (Fig. 5). Folding of the EC2 was variable, with some areas being highly folded and others having no folds (Fig. 4c and Fig. 5).

3.3. Evidence of a partial syncytium in diapause and early post-diapause development

Distinct cell membranes were apparent with light microscopy in *B. poppei* at the PN stage (Fig. 3d), but were not easily discernable in the ED or ID stages (Fig. 6). In TEM micrographs, nuclei in the ED and ID stages were often observed with no organellar structures or plasma membrane between them (Fig. 6c,d). Plasma membranes were discernable with light microscopy immediately under the embryonic cuticle in ID and ED embryos, and appeared to terminate shortly after turning inward toward the center of the embryonic cell mass (Fig. 6e-h). No definitive extracellular space was observed in TEM or light micrographs of ED or ID stages. These observations are consistent with a partially syncytial cell mass in the ED and ID stages.

3.4. Quantitative analyses of ultrastructural features during post-diapause development

In all stages, nuclei were identified by the appearance of darkly stained heterochromatin surrounded by an envelope (Fig. 7). The number of nuclei quadrupled from the ED to the PN stage (Fig. 8a; Welch ANOVA $p < 0.0097$ on $\log_{10}$ transformed data; Tukey's HSD $p < 0.0042$) and doubled from the ID to PN stage ($p < 0.0291$). The cell mass at the ED and ID stages of post-diapause development was dominated by yolk platelets. Yolk platelets decrease in abundance during early development, but were still present at the PN stage (Figs. 3, 7, 8). The total volume of yolk per animal decreased significantly during post-diapause development of *B. poppei* (Fig. 8b; Welch ANOVA on the $\log_{10}$ transformed data, $p < 0.0118$). Total yolk volume in *B. poppei* at the PN stage was approximately one-quarter of the total yolk volume contained at the ED stage ($p < 0.0059$). By contrast, the average diameter of the yolk platelets did not change substantially during early development; yolk platelet diameter was 1.59 ± 0.01 μm, 1.63 ± 0.02 μm, and 1.55 ± 0.02 μm at the ED, ID, and PN stages, respectively. These very minor differences in yolk diameter were statistically significant (One way ANOVA, $p < 0.0033$), but it was a decrease in the number of yolk platelets that caused the large decrease in total yolk volume.

3.5. Additional ultrastructural features visible during post-diapause development

In some, but not all, of the sectioned individuals for each stage of development, small uniformly electron opaque structures with spheroid shapes were observed (Fig. 9a,b). These structures were tentatively identified as lipid droplets. It was not possible to characterize changes in these structures during development, because they were often missing from sections. The presence of spherical empty spaces in sections lacking putative lipid droplets (Fig. 9c) suggests that they may have been lost in processing of sections. Structures that may be either vesicles or immature mitochondria were visible at all stages (Fig. 10). Mitochondria with clear lamellar cristae were visible at the PN stage, typically in proximity to myofibrils (Fig. 11). The myofibrils had variable ratios of actin and myosin with the majority of cross-sectional area of muscles lacking actin

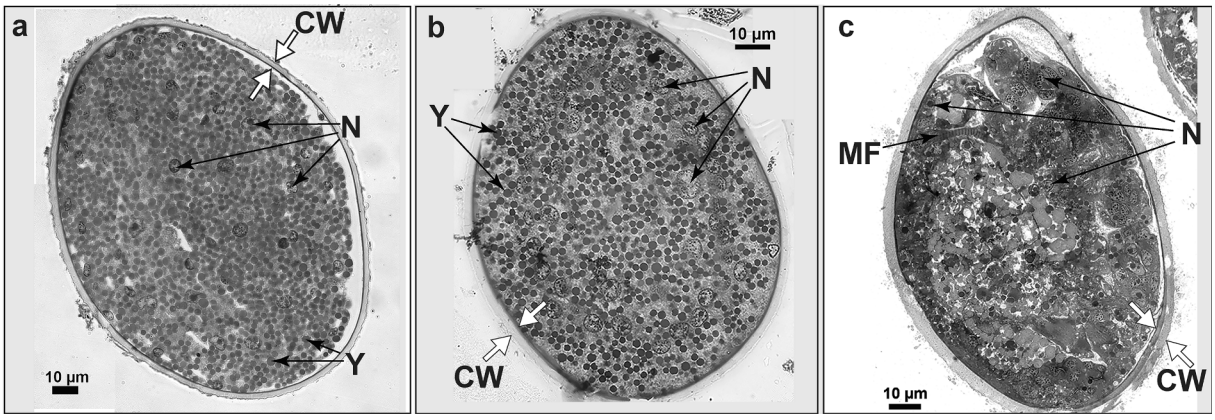

Fig. 3. Representative overview sections for post-diapause *B. poppei* at the (a) ED stage, (b) ID stage, and (c) PN stage of development. In all three stages, *B. poppei* are surrounded by a continuous cyst wall (CW; white arrows). Internal ultrastructure is dominated by yolk platelets (Y) and nuclei (N) in the ED and ID stages. Clusters of muscle fibers (MF) are only visible in the PN stage. Images reconstructed from multiple micrographs of 1 μm sections for ED and ID embryos. Multiple 0.5 μm sections were used for reconstruction of the pre-nauplius.

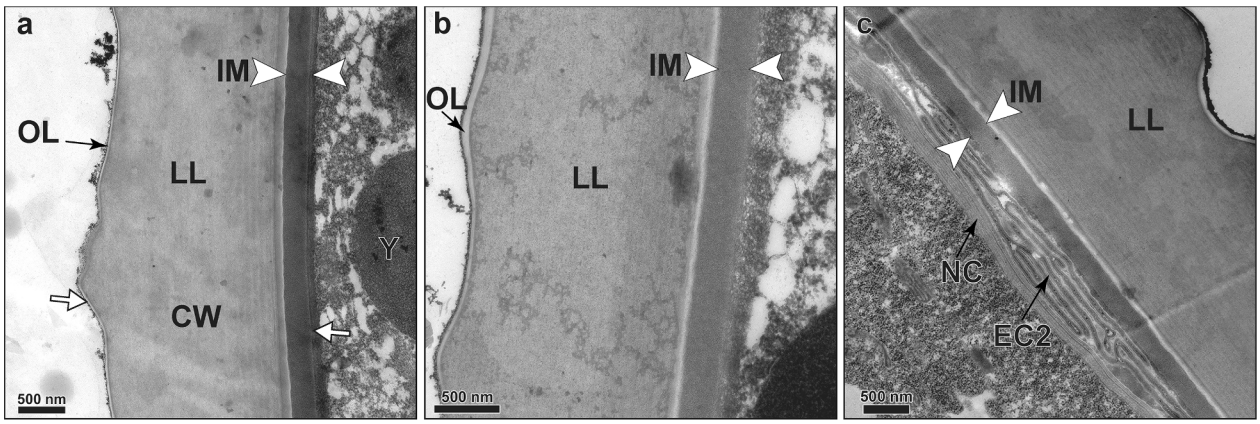

Fig. 4. Ultrastructure of the cyst wall (CW) shows little change during post-diapause development in *B. poppei*. Representative TEM images provided at the (a) ED stage, (b) ID stage, and (c) PN stage. The cyst wall is composed of three layers, the outer layer (OL), the lamellar layer (LL) and the inner membrane (IM). Two additional layers were present in the PN stage: the second embryonic cuticle (EC2) and the first naupliar cuticle (NC). All sections were 90 nm thick.

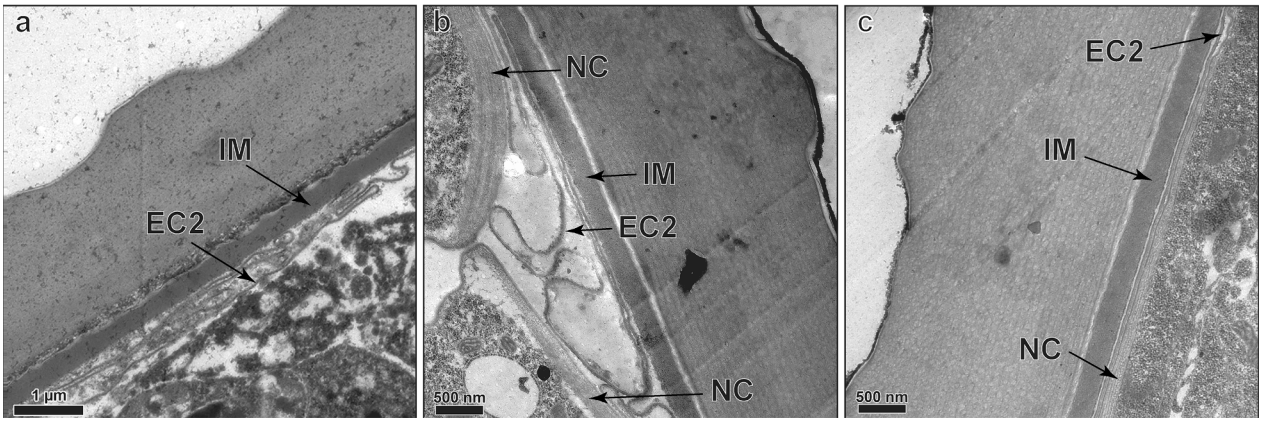

Fig. 5. The variable structure of the second embryonic cuticle in representative images of the PN stage. The second embryonic cuticle (EC2) was visible as a highly folded thin structure that appears under the IM before the naupliar cuticle is formed (a). The lamellar naupliar cuticle forms under the EC2 in the PN stage (b). In some sections, the EC2 lacked folds and was obvious only where it separated from the IM and NC (c). All sections were 90 nm thick.

(Fig. 11b). Myofibrils were not visible in the ED or ID stages (Figs. 3, 6).

4. Discussion

In order to predict the impacts of climate change and anthropogenic chemicals on maritime lakes in the Antarctic and subantarctic we must understand the most resilient life-stages of critically important species in these lakes. The copepod, *B. poppei*, is an important species in maritime lakes of the Southern Ocean, because it occupies the top of the food web and is often the only crustacean zooplankton present. The primary goal of this study was to provide an ultrastructural analysis of both the dormant embryo and post-dormancy development in *B. poppei* as a foundation for future biochemical, molecular and ecological research on resilience in the face of climate change and anthropogenic chemical pollution. To the best of the authors' knowledge, this is the first report that provides ultrastructural observations of copepod embryos present in Antarctic lake sediments, and the first to provide an ultrastructural analysis of the continuous process of post-dormancy development in any freshwater copepod. The data demonstrate that 1) the diapause embryo is a partially syncytial and appears to be a mid-stage gastrula, 2) rapid proliferation of nuclei occurs in a partially syncytial cell mass after dormancy ends, 3) 75% of yolk platelets are completely consumed prior to emergence of the nauplius larva, and 4) embryos are surrounded by a tri-layered cyst wall until the nauplius is fully formed. Schematic diagrams based on light microscopy and EM images in this work now allow the rapid identification of developmental stages described in a previous publication (Reed et al., 2018).

Few published works compare embryo structure among crustacean zooplankton, but the conserved structure of the cyst wall in diapause embryos provides insights into susceptibility to anthropogenic chemicals. The three layers of the cyst wall in *B. poppei* are similar to layers observed in other calanoid copepods (Couch et al., 2001; Cuoc et al., 1994; Dharani and Altaff, 2004; Hairston and Olds, 1984; Hirose et al., 1992; Hubble and Kirby, 2007; Ianora and Santella, 1991; Santella and Ianora, 1990), *Daphnia* (Seidman and Larsen, 1979), and *Artemia* spp. (Morris and Afzelius, 1967; Rosowski et al., 1997). The maternally derived proteinaceous coat that provides *A. franciscana* with a barrier to lipophilic chemicals (Covi et al., 2016) is not present in copepods (Ianora and Santella, 1991; Santella and Ianora, 1990) or cladocerans (Seidman and Larsen, 1979). This may be why embryos of *B. poppei* and *D. magna* are susceptible to lipophilic toxicant exposure during dormancy (Navis et al., 2013, 2015; Reed et al., 2018) while *A. franciscana* are not (Covi et al., 2016).

Comparative evaluations of the cyst wall in crustacean embryos are rare and incomplete. In the few species for which ultrastructural data exist, three to four distinct layers are present in the cyst wall of diapause embryo (Couch et al., 2001; Rosowski et al., 1997; Seidman and Larsen, 1979). The conservation of these layers in additional species and the physiological role these layers play remain uncertain in the literature. Given the extreme duration of embryonic dormancy experienced by diverse crustacean zooplankton, a cyst wall structure that protects against physical or biochemical disruption should be conserved. In

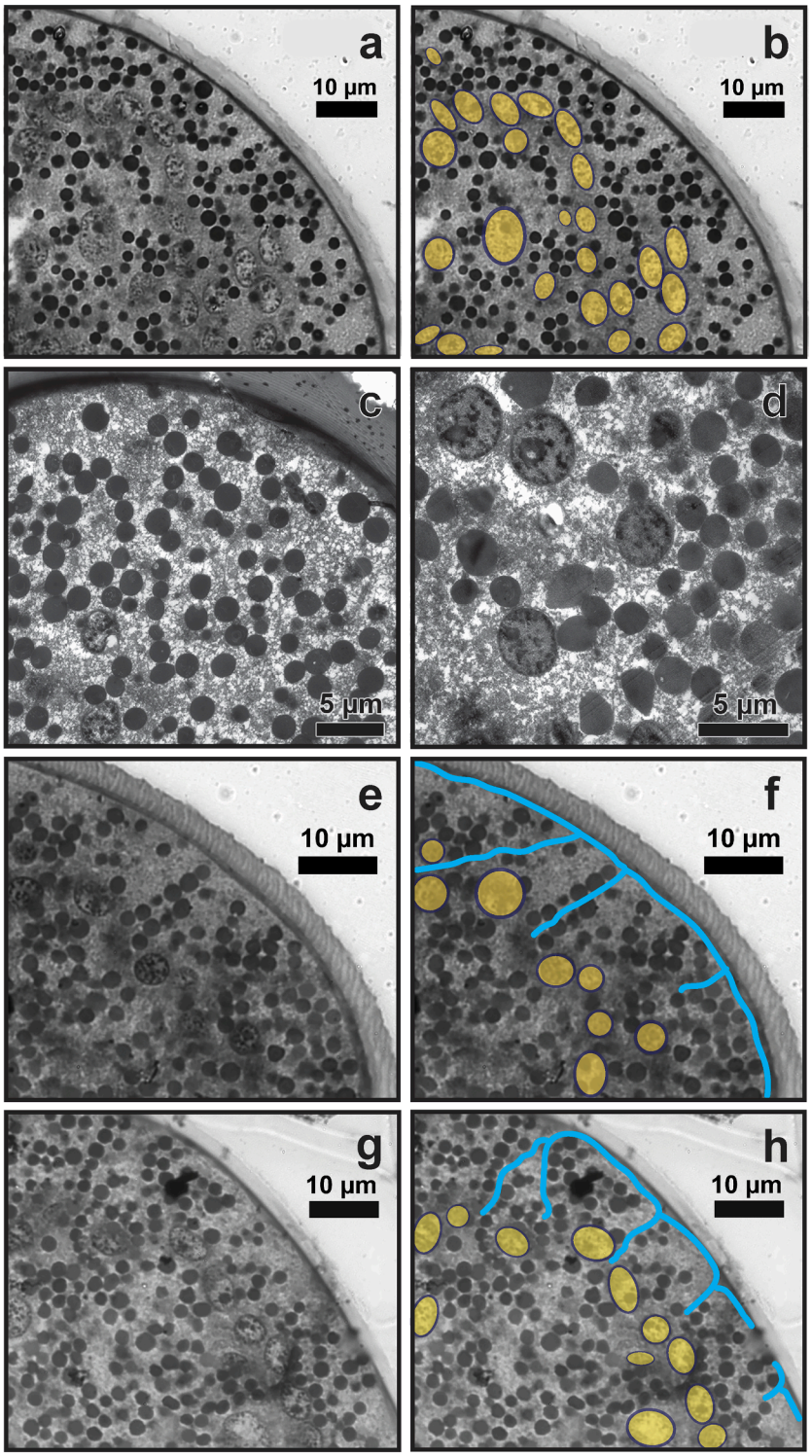

Fig. 6. Representative images demonstrating a partial syncytium in ED and ID embryos of *B. poppei*. No membranes are apparent between clustered nuclei in light micrographs of ED embryos at 100X magnification (a,b). No plasma membranes are apparent between nuclei in TEM micrographs of ED (c) or ID (d) embryos. Plasma membranes are occasionally apparent in the ED embryo immediately proximal to the cuticle, but appear to terminate as they penetrate the embryonic cell mass (e,f). A similar membrane pattern occurs in the ID embryo (g,h). Panels b, f and h are the same images as panels a, e and g, respectively; membranes, blue; nuclei, yellow. Light micrograph images reconstructed from multiple micrographs of 1 µm sections. TEM micrographs of 90 nm sections.

Artemia, the innermost of the cyst wall layers acts as a barrier to hydrophilic substances, including dissolved metals (Morris and Afzelius, 1967) and protons (Busa et al., 1982). There are no published data evaluating the function of this layer in *Boeckella*. The middle layer must confer resistance to physical stressors, because it has a thick lamellar structure similar to procuticle (Couch et al., 2001; Seidman and Larsen, 1979). This layer comprises 88% of cyst wall thickness in *B. poppei*, and 55–83% of the cyst wall of copepods for which ultrastructural data has been published (Couch et al., 2001; Cuoc et al., 1994; Dharani and Altaff, 2004; Hairston and Olds, 1984; Hirose et al., 1992; Hubble and Kirby, 2007; Ianora and Santella, 1991; Santella and Ianora, 1990). In most species, the lamellar layer accounts for >65% of cyst wall thickness. This is the largest single structure in cryptobiotic zooplankton embryos, which indicates a conserved substantial energetic investment. It is likely that the outermost layer provides protection against microbial attack during prolonged dormancy, because embryos of *B. poppei* are found in the sediment of lakes known to have expansive microbial populations (Almada et al., 2004; Butler et al., 2005). If the outer layer did not provide protection, then pitting of the cuticle by bacterial chitinases should be visible. No such pitting is noted in the literature for any

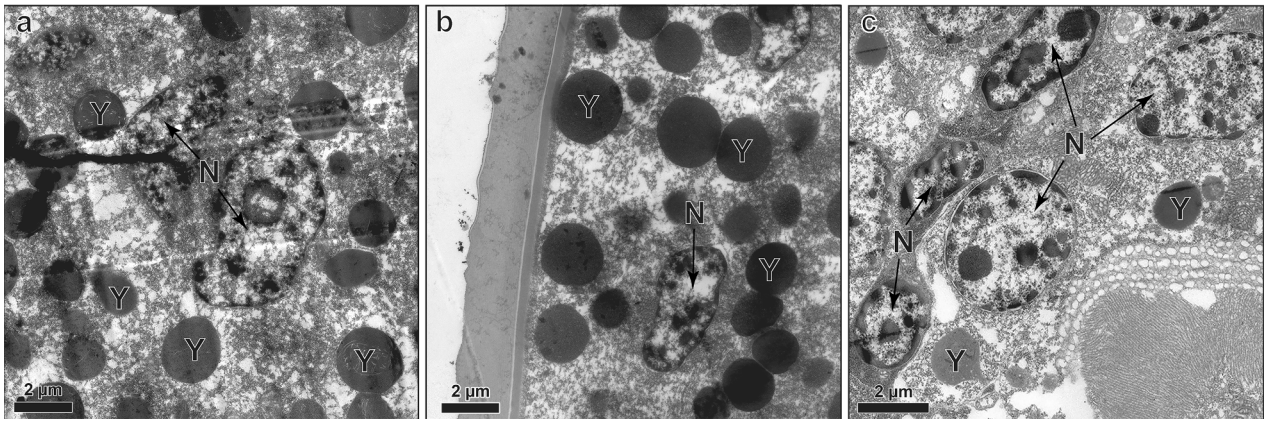

Fig. 7. Nuclei (N) were identified in TEM images by the presence of a nuclear envelope and both euchromatin and heterochromatin during post-diapause development in *B. poppei*. In (a) ED embryos and (b) ID embryos, nuclei were scattered among yolk platelets (Y). Nuclei with clear nuclear pores are visible in individuals of the (c) PN stage. All sections were 90 nm thick.

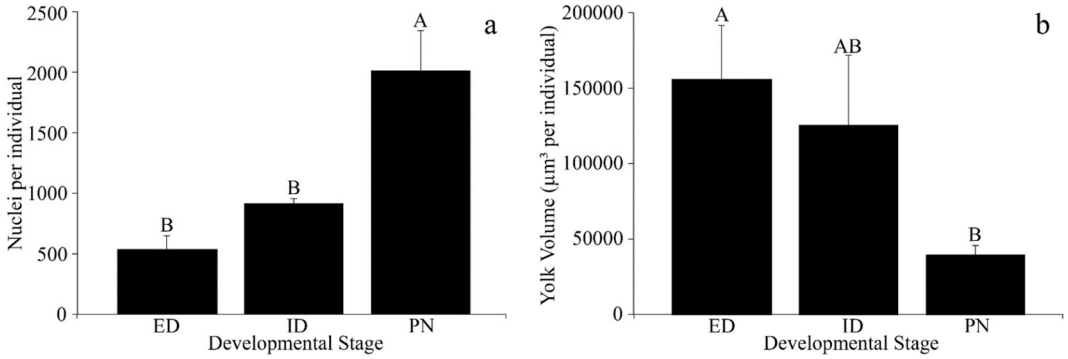

Fig. 8. Quantitative change of (a) nuclei and (b) yolk platelets during post-diapause development in *B. poppei*. Data derived from analysis of sectioned individuals, and plotted as mean of each stage ± SEM; ED (n = 5), ID (n = 4), and PN (n = 4) stage. Bars with the same letter are not significantly different (Welch ANOVA = 0.05 on $\log_{10}$ transformed data).

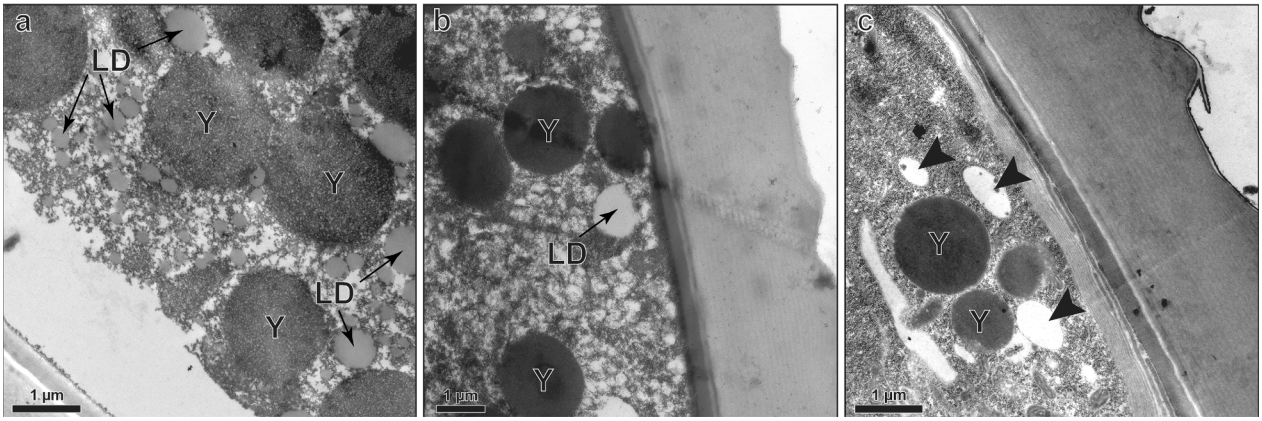

Fig. 9. Yolk platelets and lipid droplets in *B. poppei* at the (a) ED and (b) ID stages. No lipid droplets were captured in images at the PN stage, though spaces where lipid droplets may have fallen out due to the processing procedure for transmission electron microscopy were visible (c; black arrowheads). All sections were 90 nm thick.

species, and was not observed in the present study. The biochemical composition of at least three conserved layers of the cyst wall in dormant crustacean embryos should be of great interest to engineers because these layers block the movement of hydrophilic substances, provide structural integrity and appear to passively resist microbial attack.

Emergence from the encapsulating cyst wall in crustacean zooplankton gives the appearance of sequential cuticular molting, but molting regulation remains largely unstudied in zooplankton embryos. The first embryonic cuticle (EC1) is most likely the lamellar layer of the cyst wall in the diapause embryo in *B. poppei* (Couch et al., 2001). A very thin second embryonic cuticle (EC2) appears before the naupliar cuticle forms in *B. poppei* (Fig. 5) and *A. franciscana*(Rosowski et al., 1997). When the cyst wall ruptures, the EC2 expands to provide a larger space for naupliar development in *A. franciscana* (Rosowski et al., 1997), and

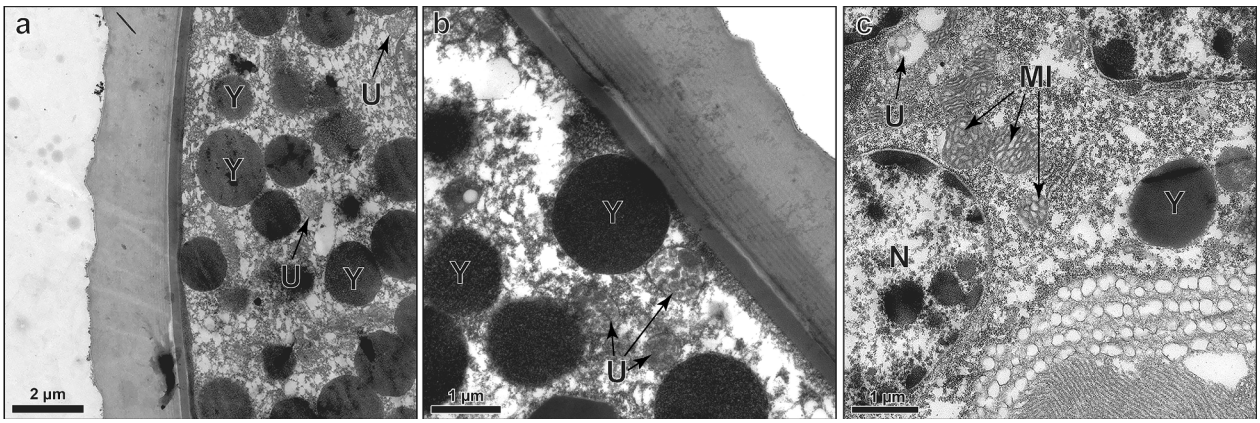

Fig. 10. Putative immature mitochondria or vesicles (U) in representative TEM images of *B. poppei* at the (a) ED stage and (b) ID stage. Yolk platelets (Y) are visible in all stages. In the (c) PN stage, well-defined mitochondria (MI) with clear lamellar cristae are visible near unknown vesicular structures with electron translucent lumens. All sections were 90 nm thick.

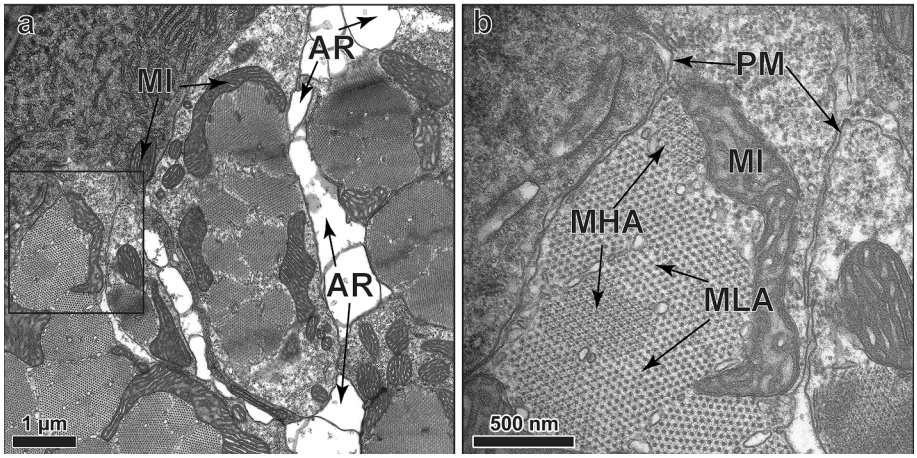

Fig. 11. Clusters of muscle fibers and numerous mitochondria (MI) are visible (a) in the Pre-Nauplius (PN) during post-diapause development. Well-defined mitochondria (b, enlargement of area in box of panel a) are often close to myofibrils. Regions of myofibril with high actin (MHA) and regions of myofibril with low actin (MLA) are visible within the same myofibril. Clear cell membranes (CM) are also visible at this stage. Both sections are 90 nm thick. Possible artifact (AR) where material appears to have fallen out during processing is visible as empty space.

lack of expansion results in malformation of the nauplius larva in this species (Neumeyer et al., 2015). The same malformation effect occurs in *D. magna* (Stout, 1956). By contrast, the nauplius of *B. poppei* is completely formed prior to rupture of the cyst wall, and expansion of the EC2 occurs immediately prior to hatching of the fully formed nauplius. In effect, the timing of molting events relative to naupliar development differs in important functional ways among crustacean zooplankton, but the molting events are conserved.

Diapause in crustacean zooplankton occurs early in embryonic development at time when the embryo is partially syncytial. The brine shrimp, *A. franciscana*, enters diapause as a partially syncytial gastrula stage embryo (Clegg and Conte, 1980). Embryos of *Daphnia* spp. also enter diapause as a partially syncytial blastula or gastrula, evidenced by superficial cleavage that leaves an ectodermal layer of cells adjacent to the cyst wall with incomplete basolateral plasma membranes (Seidman and Larsen, 1979; Stout, 1956). The ectodermal layer adjacent to the cyst wall is not syncytial immediately after release of the diapause embryo by females of the copepod, *B. triarticulata*, but plasma membranes in the yolk-rich center of the diapause embryo are missing in this species (Couch et al., 2001). By contrast, cell membranes and extracellular space are clearly visible for all cells in subitaneous eggs of the copepod, *B. triarticulata* (Couch et al., 2001). The present work demonstrates that diapause embryos of the copepod, *B. poppei*, isolated from Antarctic sediments have a syncytial structure with incomplete plasma membranes adjacent to the cuticle and no visible extracellular spaces (Fig. 6). This syncytial structure in *B. poppei* is more similar to the branchiopods, *Daphnia* and *Artemia*, than the structure reported by Couch et al. (2001) for embryos of the copepod, *B. triarticulata* immediately after release from the female. Development after diapause is broken in *B. poppei* (Fig. 3) is also very similar to the development of *D. magna* described by Stout (1956). A more detailed analysis of long-term diapause and early post-diapause embryos in *B. triarticulata* is needed to determine if this species follows the same pattern as *B. poppei* and branchiopods. It is reasonable to hypothesize that there is a regulatory advantage to entering dormancy early in development when the embryo is partially syncytial and, therefore, functionally similar to a single large cell. At the very least, a comparative evaluation of the data support the hypothesis that diapause in diverse crustacean zooplankton occurs in a partially syncytial gastrula-stage embryo.

Neither cell number nor the timing of cell division during encysted post-diapause development are conserved among crustacean zooplankton. The number of nuclei in *B. poppei* quadrupled from 539 in the ED stage to 2014 in the PN stage. This is unlike diapause embryos of *A. franciscana,* which maintain 4000 nuclei during pre-emergent development from the gastrula to the first instar nauplius larva (Nakanishi et al., 1962; Olson and Clegg, 1978). The eggs of *Daphnia magna* maintain 3500 cells during diapause, and that number increases to over 7000 cells before hatching (Chen et al., 2018). Why both total cell number and the timing of cell division relative to emergence differ greatly among crustacean zooplankton remains unclear.

The mobilization of yolk stores after prolonged dormancy puts *B. poppei* at increased risk to impacts from anthropogenic chemicals. Approximately 75% of yolk platelets are completely consumed during preemergent development in *B. poppei* while 25% are left

untouched. A similar reliance on yolk occurs in *Artemia* (Warner et al., 1972) and marine copepods (Romano et al., 1996). Lipid droplets are also consumed during the development of zooplankton, but technical challenges prevented tracking of lipid consumption in *B. poppei* in the present work (Fig. 9). Dormant embryos of the anostracan, *A. franciscana*, contain diverse lipophilic chemicals, most likely from maternal partitioning (Neumeyer et al., 2015). Copepods and cladocerans continue to passively accumulate lipophilic chemicals while dormant, because they lack a barrier to these compounds (Navis et al., 2015; Reed et al., 2018). As is well documented for vertebrates (La Merrill et al., 2013), chemicals partition to lipid stores in crustaceans (Evans et al., 1982; McManus et al., 1983). Release of these chemicals when lipids are mobilized could disrupt development or emergence. Therefore, the authors recommend monitoring of lipophilic chemicals in Antarctic lakes with endemic crustacean zooplankton.

Total yolk volume and platelet abundance decreased during post-diapause development in *B. poppei* while the diameter of yolk platelets did not change. This suggests that the activation of yolk platelet consumption occurs in an all or nothing manner where an individual platelet is rapidly consumed when the process is activated. The biochemical composition of yolk platelets and the regulation of yolk mobilization in *B. poppei* warrant further investigation. It is highly unlikely that yolk stores are used to support metabolic processes during cryptobiotic dormancy, because 1. the vast majority of yolk must be preserved to support early development (Fig. 8b) and 2. embryos of this species survive nearly 200 years in the cryptobiotic state (Jiang et al., 2012).

In all stages of *B. poppei,* structures that resemble immature mitochondria or vesicles are present. The unknown structures in the ED and ID stage of *B. poppei* embryos show a membrane bound granular appearance similar to structures identified as vesicles in marine copepod embryos (Ianora and Santella, 1991; Santella and Ianora, 1990). In embryos of *B. poppei* at the PN stage, mature mitochondria were present near some of these unknown structures. Immature mitochondria often appear as spherical membrane bound structures with electron opaque appearance without clear lamellar cristae (Schmitt et al., 1973). Further work is required to conclusively identify these structures.

Muscle fibers first appear during the PN stage in *B. poppei*, and actin: myosin ratios are surprisingly variable within individual muscle fibers before hatching (Fig. 11). Actin filaments form before myosin during muscle development in vertebrates (Sanger et al., 2016), but actin is the myofibrillar component that is missing from much of the muscle in the developing nauplius larva (Fig. 11). Preferential loss of thin filaments occurs during atrophy of claw muscle in decapods (Mykles and Skinner, 1981), but selective degradation of actin after development of muscle fibers in *B. poppei* seems unlikely. A low actin:myosin ratio due to disuse seems more likely. Certainly, copepod embryos provide a new and potentially valuable model for the study of muscle development in crustaceans. Muscle mass in crustaceans is regulated by myostatin and mTOR signaling systems (Covi et al., 2010; MacLea et al., 2012), so these are two promising targets for molecular studies of muscle development in zooplankton.

5. Conclusions

This study presents the first ultrastructural investigation of post-diapause development to the first instar larva for an Antarctic freshwater copepod. Diapausing embryos of *B. poppei* are surrounded by a tri-layered cyst wall that protects the organism until a fully formed nauplius is ready to emerge. A comparison with published data indicates that this tri-layer structure is conserved in crustacean zooplankton that employ embryonic dormancy, but the timing of emergence with naupliar development is not conserved. Unlike many species of crustacean zooplankton, emergence and hatching occur in rapid succession in *B. poppei*, which allows the developing organism to remain behind the protective cyst wall until the nauplius is fully formed. This work is the first to confirm that diapause in a copepod occurs in a partially syncytial gastrula stage. A novel analysis of the literature indicates that dormancy in a partially syncytial gastrula is very likely an ancestral characteristic for crustacean zooplankton. Research on additional species is required to evaluate the potential physiological and evolutionary benefits of entering dormancy in a partially syncytial state. Much like *A. franciscana* and *D. magna,* yolk is not depleted during dormancy in *B. poppei*. Instead, yolk is reserved to fuel cell division and differentiation after dormancy ends. If anthropogenic chemicals partition to the yolk structures, it is likely that *B. poppei* embryos will show physiological manifestations of these chemicals when yolk is mobilized during pre-emergent development. In laboratory studies, this would appear as low hatching success. In ecological studies, this would appear as a disconnect between larval abundance in the Austral spring and adult fecundity in the preceding Austral summer.

CRediT authorship contribution statement

Katherine A. Reed: Conceptualization, Formal analysis, Investigation, Methodology, Validation, Visualization, Writing - original draft, Writing - review & editing. **Sung Gu Lee:** Formal analysis, Funding acquisition, Investigation, Project administration, Resources, Writing - review & editing. **Jun Hyuck Lee:** Funding acquisition, Writing - review & editing. **Hyun Park:** Funding acquisition, Project administration, Writing - review & editing. **Joseph A. Covi:** Conceptualization, Data curation, Formal analysis, Funding acquisition, Investigation, Methodology, Project administration, Resources, Supervision, Writing - original draft, Writing - review & editing.

Declaration of Competing Interest

The authors declare that they have no known competing financial interests or personal relationships that could have appeared to influence the work reported in this paper.

Acknowledgements

Grant support for this project was provided by the Korea Polar Research Institute (KOPRI) Grant PE20040. Access to shipping logistics with DAMCO was provided by the National Science Foundation Office of Polar Programs, United States Antarctic Program. The authors thank Dr. Alison Taylor and Mark Gay for technical training and consultation in Electron Microscopy. Electron Microscopy was conducted in the UNCW Richard Dillaman Biological Imaging Facility at UNCW. The authors thank Yanina Ciriani for field assistance.

Appendix A. Supplementary data

Supplementary data to this article can be found online at https://doi.org/10.1016/j.jsb.2021.107705.

References

Alekseev, V.R., DeStasio, B., Gilber, J.J., 2007. Diapause in aquatic invertebrates: theory and human use. Springer Science and Business Media.
Almada, P., Allende, L., Tell, G., Izaguirre, I., 2004. Experimental evidence of the grazing impact of Boeckella poppei on phytoplankton in a maritime Antarctic lake. Polar Biol. 28, 39–46.
Bayly, I., Gibson, J., Wagner, B., Swadling, K., 2003. Taxonomy, ecology and zoogeography of two East Antarctic freshwater calanoid copepod species: Boeckella poppei and Gladioferens antarcticus. Antarct. Sci. 15, 439–448.
Bayly, I.A.E., 1995. Distinctive aspects of the zooplankton of large lakes in Australasia, Antarctica and South America. Mar. Freshwater Res. 46, 1109–1120.
Brendonck, L., De Meester, L., 2003. Egg banks in freshwater zooplankton: evolutionary and ecological archives in the sediment. Hydrobiol. 491, 65–84.
Briski, E., Bailey, S.A., MacIsaac, H.J., 2013. Separation strategies for invertebrate dormant stages contained in sediment. Aquat. Biol. 18, 209–215.

Burns, W.A., 1978. Thick Sections: Technique and applications, in Diagnostic Electron Microscopy. John Wiley & Sons, New York.
Busa, W.B., Crowe, J.H., Matson, G.B., 1982. Intracellular pH and the metabolic status of dormant status of dormant and developing Artemia embryos. Arch. Biochem. Biophys. 216, 711–718.
Butler, H., Atkinson, A., Gordon, M., 2005. Omnivory and predation impact of the calanoid copepod Boeckella poppei in a maritime Antarctic lake. Polar Biol. 28, 815–821.
Cáceres, C.E., Hairston, N.G., 1998. Benthic-pelagic coupling in planktonic crustaceans: the role of the benthos. Adv. Limnol., Vol 52: Evolutionary and Ecological Aspects of Crustacean Diapause 52, 163-174.
Chen, F., Marcus, N.H., 1997. Subitaneous, diapause, and delayed-hatching eggs of planktonic copepods from the northern Gulf of Mexico: Morphology and hatching success. Mar. Biol. 127, 587–597.
Chen, L.X., Barnett, R.E., Horstmann, M., Bamberger, V., Heberle, L., Krebs, N., Colbourne, J.K., Gómez, R., Weiss, L.C., 2018. Mitotic activity patterns and cytoskeletal changes throughout the progression of diapause developmental program in Daphnia. BMC Cell Biol. 19, 12.
Clegg, J., Conte, F., 1980. Cellular and developmental biology of Artemia. The Brine Shrimp Artemia, Whitteren, Belgium.
Clegg, J.S., Drinkwater, L.E., Sorgeloos, P., 1996. The metabolic status of diapause embryos of Artemia franciscana (SFB). Physiol. Zool. 69, 49–66.
Couch, K.M., Downes, M., Burns, C.W., 2001. Morphological differences between subitaneous and diapause eggs of Boeckella triarticulata (Copepoda:Calanoida). Freshw. Biol. 46, 925–933.
Covi, J.A., Bader, B.D., Chang, E.S., Mykles, D.L., 2010. Molt cycle regulation of protein synthesis in skeletal muscle of the blackback land crab, Gecarcinus lateralis, and the differential expression of a myostatin-like factor during atrophy induced by molting or unweighting. J. Exp. Biol. 213, 172–183.
Covi, J.A., Hutchison, E.R., Neumeyer, C.H., Gunderson, M.D., 2016. Rotenone decreases hatching success in brine shrimp embryos by blocking development: Implications for zooplankton egg banks. PloS One. 11, 17.
Cuoc, C., Brunet, M., Arnaud, J., Mazza, J., 1994. Formation of egg envelopes in the fresh-water calanoid copepod Hemidiaptomus ingens. Invertebr. Reporod. Dev. 26, 63–78.
Dharani, G., Altaff, K., 2004. Ultra-structure of subitaneous and diapausing eggs of planktonic copepod Sinodiaptomus (Rhinediaptomus) indicus. Curr. Sci. 87, 109–112.
Díaz, A., Maturana, C.S., Boyero, L., Escalante, P.D., Tonin, A.M., Correa-Araneda, F., 2019. Spatial distribution of freshwater crustaceans in Antarctic and Subantarctic lakes. Sci. Rep. 9, 8.
Evans, M.S., Bathelt, R.W., Rice, C.P., 1982. PCBs and other toxicants in Mysis relicta. Hydrobiol. 93, 205–215.
Hairston, N.G., Cáceres, C.E., 1996. Distribution of crustacean diapause: Micro- and macroevolutionary pattern and process. Hydrobiol. 320, 27–44.
Hairston, N., Kearns, C., 2002. Temporal dispersal: Ecological and evolutionary aspects of zooplankton egg banks and the role of sediment mixing. Integr. Comp. Biol. 42, 481–491.
Hairston, N.G., Olds, E.J., 1984. Population differences in the timing of diapause - adaptation in a spatially heterogenous environment. Oecologia. 61, 42–48.
Hand, S., Podrabsky, J., 2000. Bioenergetics of diapause and quiescence in aquatic animals. Thermochim. Acta 349, 31–42.
Hirose, E., Toda, H., Saito, Y., Watanabe, H., 1992. Formation of the multiple-layered fertilization envelope in the embryo of Calanus sinicus Brodsky (Copepoda, Calanoida). J. Crust. Biol. 12, 186–192.
Hubble, S.K., Kirby, R.R., 2007. Transmission electron microscopy of marine crustacean eggs. Crustaceana. 80, 739–745.
Ianora, A., Santella, L., 1991. Diapause embryos in the neustonic copepod Anomalocera patersoni. Mar. Biol. 108, 387–394.
Izaguirre, I., Allende, L., Marinone, M.C., 2003. Comparative study of the planktonic communities of three lakes of contrasting trophic status at Hope Bay (Antarctic Peninsula). J. Plankton Res. 25, 1079–1097.
Jiang, X., Zhao, S., Xu, Z., Wang, G., He, J., Cai, M., 2012. Abundance and age of viable resting eggs of the calanoid copepod Boeckella poppei Mrázek in sediments: evidence of egg banks in two Antarctic maritime lakes. Polar Biol. 35, 1525–1531.
La Merrill, M., Emond, C., Kim, M.J., Antignac, J.P., Le Bizec, B., Clement, K., Birnbaum, L.S., Barouki, R., 2013. Toxicological function of adipose tissue: Focus on persistent organic pollutants. Environ. Health Perspect. 121, 162–169.
Laybourn-Parry, J., 2003. Polar limnology, the past, the present and the future. In: Huiskes, A. (Ed.), Antarctic Biology in a Global Context. Blackhuys Publishers, Leiden, The Netherlands, pp. 321–329.
Laybourn-Parry, J., Pearce, D.A., 2007. The biodiversity and ecology of Antarctic lakes: models for evolution. Phil. Trans. R. Soc. B. 362, 2273–2289.
MacLea, K.S., Abuhagr, A.M., Pitts, N.L., Covi, J.A., Bader, B.D., Chang, E.S., Mykles, D. L., 2012. Rheb, an activator of target of rapamycin, in the blackback land crab, Gecarcinus lateralis: cloning and effects of molting and unweighting on expression in skeletal muscle. J. Exp. Biol. 215, 590–604.
Marcus, N.H., Boero, F., 1998. Minireview: The importance of benthic-pelagic coupling and the forgotten role of life cycles in coastal aquatic systems. Limnol. Oceanogr. 43, 763–768.
Marcus, N.H., Lutz, R., Burnett, W., Cable, P., 1994. Age, viability, and vertical distribution of zooplankton resting eggs from an anoxic basin - evidence of an egg bank. Limnol. Oceanogr. 39, 154–158.
Maturana, C.S., Rosenfeld, S., Naretto, J., Convey, P., Poulin, E., 2019. Distribution of the genus Boeckella (Crustacea, Copepoda, Calanoida, Centropagidae) at high latitudes in South America and the main Antarctic biogeographic regions. ZooKeys 1–15.
McManus, G.B., Wyman, K.D., Peterson, W.T., Wurster, C.F., 1983. Factors affecting the elimination of PCBs in the marine copepod Acartia tonsa. Estuar. Coast. Shelf Sci. 17, 421–430.
Morris, J.E., Afzelius, B.A., 1967. The structure of the shell and outer membranes in encysted Artemia salina embryos during cryptobiosis and development. J. Ultrastruct. Res. 20, 244–259.
Mykles, D.L., Skinner, D.M., 1981. Preferential loss of thin-filaments during molt-induced atrophy in crab claw muscle. J. Ultrastruct. Res. 75, 314–325.
Nakanishi, Y.H., Iwasaki, T., Okigaki, T., Kato, H., 1962. Cytological Studies of Artemia salina I. Embryonic development without cell multiplication after the blastula stage in encysted dry eggs. Annot. Zool. Jpn. 35, 223–228.
Navis, S., Waterkeyn, A., Voet, T., De Meester, L., Brendonck, L., 2013. Pesticide exposure impacts not only hatching of dormant eggs, but also hatchling survival and performance in the water flea Daphnia magna. Ecotoxicol. 22, 803–814.
Navis, S., Waterkeyn, A., Putman, A., De Meester, L., Vanermen, G., Brendonck, L., 2015. Timing matters: Sensitivity of Daphnia magna dormant eggs to fenoxycarb exposure depends on embryonic developmental stage. Aquat. Toxicol. 159, 176–183.
Neumeyer, C.H., Gerlach, J.L., Ruggiero, K.M., Covi, J.A., 2015. A novel model of early development in the brine shrimp, Artemia franciscana, and its use in assessing the effects of environmental variables on development, emergence, and hatching. J. Morphol. 276, 342–360.
Olson, C.S., Clegg, J.S., 1978. Cell division during the development of Artemia salina. Wilhelm Roux's Archives 184, 1–13.
Pociecha, A., Dumont, H.J., 2008. Life cycle of Boeckella poppei Mrazek and Branchinecta gaini Daday (King George Island, South Shetlands). Polar Biol. 31, 245–248.
Reed, K.A., Park, H., Lee, S.G., Lee, W., Lee, S.H., Bleau, J.M., Munden, T.N.M., Covi, J. A., 2018. Embryos of an Antarctic zooplankton require anoxia for dormancy, are permeable to lipophilic chemicals, and reside in sediments containing PCBs. Sci. Rep. 8, 13.
Reynolds, E., 1963. The use of lead citrate at high pH as an electron-opaque stain in electron microscopy. J. of Cell Biol. 17, 208–212.
Romano, G., Ianora, A., Santella, L., Miralto, A., 1996. Respiratory metabolism during embryonic subitaneous and diapause development in Pontella mediterranea (Crustacea, Copepoda). J. Comp. Physiol. B. 166, 157–163.
Rosowski, J.R., Belk, D., Gouthro, M.A., Lee, K.W., 1997. Ultrastructure of the cyst shell and underlying membranes of the brine shrimp Artemia franciscana Kellogg (Anostraca) during postencystic development, emergence, and hatching. J. Shellfish Res. 16, 233–249.
Sanger, J.W., Wang, J., Fan, Y., White, J., Mi-Mi, L., Dube, D.K., Sanger, J., Bruyne, D., 2016. Assembly and maintenance of myofibrils in striated muscle in the actin cytoskeleton. In: Barrett, J.E. (Ed.), Handbook of Experimental Pharmacology. Philadelphia.
Santella, L., Ianora, A., 1990. Subitaneous and diapause eggs in Mediterranean populations of Pontella mediterranea (Copepoda, Calanoida) - a morphological study. Mar. Biol. 105, 83–90.
Schindelin, J., Arganda-Carreras, I., Frise, E., Kaynig, V., Longair, M., Pietzsch, T., Preibisch, S., Rueden, C., Saalfeld, S., Schmid, B., Tinevez, J.Y., White, D.J., Hartenstein, V., Eliceiri, K., Tomancak, P., Cardona, A., 2012. Fiji: an open-source platform for biological-image analysis. Nat. Methods 9, 676–682.
Schmitt, H., Grossfeld, H., Littauer, U.Z., 1973. Mitochondrial Biogenesis During Differentiation of Artemia-salina cysts. J. Cell Biol. 58, 643–649.
Seidman, L.A., Larsen, J.H., 1979. Ultrastructure of the envelopes of resistant and non-resistant Daphnia eggs. Can. J. Zool. 57, 1773–1777.
Spurr, A.R., 1969. A low-viscosity epoxy resin embedding medium for electron microscopy. J. Ultrastruct. Res. 26 (1–2), 31–43.
Stout, V.M., 1956. The development of Daphnia magna. Doctoral Dissertation, Bedford College, University of London.
Sugumar, V., Munuswamy, N., 2006. Ultrastructure of cyst shell and underlying membranes of three strains of the brine shrimp Artemia (Branchiopoda : Anostraca) from South India. Microsc. Res. Tech. 69, 957–963.
Warner, A.H., Puodziukas, J.G., Finamore, F.J., 1972. Yolk platelets in brine shrimp embryos: Site of biosynthesis and storage of the diguanosine nucleotides. Exp. Cell. Res. 70, 365–375.